

Atmospheric residence time of ^{210}Pb determined from the activity ratios with its daughter radionuclides ^{210}Bi and ^{210}Po



P. Semertzidou*, G.T. Piliposian, P.G. Appleby

Environmental Radioactivity Research Centre, Department of Mathematical Sciences, University of Liverpool, UK

ARTICLE INFO

Article history:

Received 4 September 2015
Received in revised form
12 April 2016
Accepted 16 April 2016
Available online 29 April 2016

Keywords:

^{210}Pb
Atmospheric residence time
 $^{210}\text{Bi}/^{210}\text{Pb}$ activity ratio
 $^{210}\text{Po}/^{210}\text{Pb}$ activity ratio
Reservoir effect of the stratosphere

ABSTRACT

The residence time of ^{210}Pb created in the atmosphere by the decay of gaseous ^{222}Rn is a key parameter controlling its distribution and fallout onto the landscape. These in turn are key parameters governing the use of this natural radionuclide for dating and interpreting environmental records stored in natural archives such as lake sediments. One of the principal methods for estimating the atmospheric residence time is through measurements of the activities of the daughter radionuclides ^{210}Bi and ^{210}Po , and in particular the $^{210}\text{Bi}/^{210}\text{Pb}$ and $^{210}\text{Po}/^{210}\text{Pb}$ activity ratios. Calculations used in early empirical studies assumed that these were governed by a simple series of equilibrium equations. This approach does however have two failings; it takes no account of the effect of global circulation on spatial variations in the activity ratios, and no allowance is made for the impact of transport processes across the tropopause. This paper presents a simple model for calculating the distributions of ^{210}Pb , ^{210}Bi and ^{210}Po at northern mid-latitudes (30° – 65°N), a region containing almost all the available empirical data. By comparing modelled $^{210}\text{Bi}/^{210}\text{Pb}$ activity ratios with empirical data a best estimate for the tropospheric residence time of around 10 days is obtained. This is significantly longer than earlier estimates of between 4 and 7 days. The process whereby ^{210}Pb is transported into the stratosphere when tropospheric concentrations are high and returned from it when they are low, significantly increases the effective residence time in the atmosphere as a whole. The effect of this is to significantly enhance the long range transport of ^{210}Pb from its source locations. The impact is illustrated by calculations showing the distribution of ^{210}Pb fallout versus longitude at northern mid-latitudes.

© 2016 Elsevier Ltd. All rights reserved.

1. Introduction

The natural radionuclide ^{210}Pb is widely used for dating and interpreting environmental records stored in natural archives such as lake or marine sediments and peat bogs. Since the source of the ^{210}Pb is atmospheric fallout, models of the processes controlling its distribution in the atmosphere and subsequent deposition onto the Earth's surface are of considerable importance to this work. Outputs from the atmospheric model become inputs to models of the transport processes by which fallout deposited on the landscape accumulates in the sediment record. These terrestrial and aquatic models are of fundamental importance to the ^{210}Pb dating methodology. They are also essential to the use of sediment records for reconstructing historical levels of atmospheric pollution by e.g. heavy metals (lead and mercury) and persistent organic pollutants

(POPs). Use of ^{210}Pb as a tracer for establishing the validity of these models requires good estimates of the atmospheric ^{210}Pb flux. Good estimates of the ^{210}Pb flux are also necessary to a reliable interpretation of ^{210}Pb dating calculations. Atmospheric models of ^{210}Pb are also of considerable interest to studies of global circulation and the long-range transport of atmospheric pollutants. The source of ^{210}Pb is well-known and relatively constant on timescales of a year or more. It is thus an ideal tracer for studying atmospheric processes on these longer timescales (Baskaran, 2011; Rehfeld and Heiman, 1995).

One of the key parameters controlling the distribution of ^{210}Pb over the Earth's surface is its residence time in the atmosphere. This has been estimated using a number of different methods. One of the earliest estimates (Burton and Stewart, 1960) used two different approaches. The first, based on mass balance arguments for the ^{210}Pb inventory of a vertical column of air at Harwell in the UK, suggested a tropospheric residence time of around 17 days. The second, based on the activity ratios of ^{210}Pb and its grand-daughter

* Corresponding author.

E-mail address: semertg@liv.ac.uk (P. Semertzidou).

radionuclide ^{210}Po , suggested values of 36 days from measurements in surface air at Harwell and 22–29 days from measurements on rainwater samples. Further measurements of the $^{210}\text{Po}/^{210}\text{Pb}$ activity ratio in surface air at Harwell carried out by Peirson et al. (1966) yielded a residence time of around 40 days. Since the measured values or ratios on which these calculations were based are unlikely to be representative of the atmosphere as a whole, and the equilibrium assumptions on which they were based unlikely to be realised, the validity of these results is highly uncertain.

Similar calculations were carried out by Poet et al. (1972) using the $^{210}\text{Bi}/^{210}\text{Pb}$ and $^{210}\text{Po}/^{210}\text{Pb}$ activity ratios in surface air and precipitation at Boulder, Colorado, and by Moore et al. (1973) using the ^{222}Rn , ^{210}Pb , ^{210}Bi and ^{210}Po activity ratios in tropospheric and lower stratospheric air at a range of continental sites over the United States. Residence times were calculated by assuming that the measured activities of ^{210}Pb and its daughters arise from the decay of ^{222}Rn in the atmosphere, and that their production and removal from the atmosphere are in steady state equilibrium. The parent/daughter relationship in the decay series was expressed by the equation

$$\dot{N}_2 = \lambda_1 N_1 - \lambda_2 N_2 - k N_2 = 0$$

where N_1 and N_2 are the numbers of atoms of the parent and daughter, λ_1 and λ_2 their radioactive decay constants, and k a first order rate constant for the removal of aerosols from the atmosphere. ^{210}Pb atoms are highly reactive and quickly attached to aerosol particles. It is reasonable therefore to suppose that the daughters are similarly attached and subject to the same removal rates.

Radionuclides are usually measured in terms of their activities (disintegrations per unit time), defined by $A_1 = \lambda_1 N_1$, $A_2 = \lambda_2 N_2$. In these terms the above equation becomes

$$\dot{A}_2 = \lambda_2 \dot{N}_2 = \lambda_2 (\lambda_1 N_1 - \lambda_2 N_2 - k N_2) = \lambda_2 (A_1 - A_2) - k A_2 = 0.$$

Applying this to ^{210}Pb and its daughters, the relationships between them will be governed by the equations

$$\left. \begin{aligned} \lambda_{\text{Bi}}(A_{\text{Pb}} - A_{\text{Bi}}) - k A_{\text{Bi}} &= 0 \\ \lambda_{\text{Po}}(A_{\text{Bi}} - A_{\text{Po}}) - k A_{\text{Po}} &= 0 \end{aligned} \right\} \quad (1)$$

where A_{Pb} , A_{Bi} and A_{Po} are the activities and λ_{Pb} , λ_{Bi} , λ_{Po} their radioactive decay constants. Rearranging, the activity ratios will satisfy the equations (c.f. Moore et al., 1973):

$$\frac{A_{\text{Bi}}}{A_{\text{Pb}}} = \frac{\lambda_{\text{Bi}}}{\lambda_{\text{Bi}} + k}, \quad \frac{A_{\text{Po}}}{A_{\text{Pb}}} = \frac{\lambda_{\text{Po}} \lambda_{\text{Bi}}}{(\lambda_{\text{Po}} + k)(\lambda_{\text{Bi}} + k)} \quad (2)$$

Given the activity ratios, each of these equations can be solved to yield a value for the removal rate k . The ^{210}Pb residence time will be $T = 1/k$ (or $\ln 2/k$ depending on the preferred convention). A similar approach was adopted by Gavini et al. (1974) who measured ^{210}Pb , ^{210}Bi and ^{210}Po activity ratios in rain samples from Fayetteville, Arkansas, and by Carvalho (1995) who measured their concentrations in surface air at Lisbon, Portugal.

Table 1 summarises mean values of the ^{210}Pb residence time calculated from the $^{210}\text{Bi}/^{210}\text{Pb}$ and $^{210}\text{Po}/^{210}\text{Pb}$ activity ratios in surface air and rainwater from the above studies. Possible causes of the large discrepancy between residence times calculated from $^{210}\text{Bi}/^{210}\text{Pb}$ ratios and those calculated from $^{210}\text{Po}/^{210}\text{Pb}$ ratios were thought to be inputs of older stratospheric air, or contamination by dust particles containing ^{210}Pb , ^{210}Bi and ^{210}Po in secular equilibrium (Poet et al., 1972; Gavini et al., 1974). Assuming the main cause to be dust contamination, Poet et al. (1972) corrected their

estimates of the mean atmospheric residence time to ~4 days for particles in the lower troposphere and ~7 days for particles in precipitation. Using various arguments, Gavini et al. (1974) suggested mean residence times of ~30 days for aerosols in the troposphere and ~1 year for the stratosphere. While some of the reasons advanced may be factors, the main cause of error is almost certainly failure of the ^{210}Pb , ^{210}Bi and ^{210}Po activities in the samples to satisfy the equilibrium conditions implicit in equation (1). Since the concentrations of these radionuclides vary considerably with both geographical location and altitude, it is likely that their ratios will show similar variations. The main objective of this research is to model these variations and match the results to empirical data. This will provide a more accurate estimate of the ^{210}Pb atmospheric residence time, while also producing a simple yet reliable model of the distribution of fallout ^{210}Pb over the landscape.

2. Model equations and assumptions

The radioactive gas ^{222}Rn enters the atmosphere via exhalation from the land surface. Its subsequent distribution in the atmosphere is controlled by processes of advection, diffusion, and radioactive decay. The distributions of the ^{222}Rn daughters ^{210}Pb , ^{210}Bi and ^{210}Po are also influenced by the process of fallout. On short time-scales (hours or days), these processes can only be accurately described by using detailed 3-dimensional models (e.g. Feichter et al., 1991; Liu et al., 2001). Such models suffer from two major disadvantages, they are very computationally intensive, and over many parts of the world there is very little empirical data against which they can be validated. They are also highly dependent on the extent to which the processes and parameterizations on which they are based are accurate representations of real world processes. An international workshop (Rasch et al., 2000) comparing different global models found that they produced significantly different results for the atmospheric distribution of ^{210}Pb .

On longer time-scales (time-averaged over a year or more), some of the essential features of the available empirical data have been captured using simpler models in which conservation principles are applied to a notional vertical column of air moving horizontally over the Earth's surface, with little net transfer between adjacent columns (Jacobi and André, 1963; Turekian et al., 1977). Piliiposian and Appleby (2003) presented a more detailed model that took account of the vertical distribution of ^{222}Rn and ^{210}Pb in the atmosphere. Here we extend that work to include distributions of the ^{210}Pb daughters ^{210}Bi and ^{210}Po , and the $^{210}\text{Bi}/^{210}\text{Pb}$ and $^{210}\text{Po}/^{210}\text{Pb}$ ratios used in studies of atmospheric residence times.

2.1. Mass balance equations and models

In view of the potential complexity in solving these simplified equations, it will be useful to consider first the associated mass balance equations. Apart from providing some justification of the validity of the simplified model, they can also be used as a means for checking the validity of the numerical solutions.

If F denotes the mean global flux (per unit area) of ^{222}Rn from the Earth's land surfaces, the mean supply rate to the atmosphere as a whole will be $A_L F$ where A_L is the effective area of the Earth's land surface contributing to this flux. The global ^{222}Rn inventory in the atmosphere with activity denoted by Q_{Rn} will satisfy the balance equation

$$\dot{Q}_{\text{Rn}} = A_E \mathcal{F} - \lambda_{\text{Rn}} Q_{\text{Rn}} \quad (3)$$

The global inventory of the ^{222}Rn daughter ^{210}Pb , the activity of

Table 1
Atmospheric residence times calculated from ^{210}Pb , ^{210}Bi and ^{210}Po activity ratios in surface air and rainwater.

	Residence time from		Location	Reference
	$^{210}\text{Bi}/^{210}\text{Pb}$	$^{210}\text{Po}/^{210}\text{Pb}$		
Surface air	5 d	24 d	Boulder, Co	Poet et al., 1972
	9 d	24 d	Continental USA	Moore et al., 1973
	6 d	33 d	Lisbon, Portugal	Carvalho 1995
		36 d	Chilton, UK	Burton and Stewart 1960
		40 d	Chilton, UK	Peirson et al., 1966
Rainwater	8 d	19 d	Boulder, Co	Poet et al., 1972
	17 d	32 d	Fayetteville, Ark	Gavini et al., 1974
		22–29 d	Chilton, UK	Burton and Stewart 1960

which is denoted by Q_{pb} , will similarly satisfy the balance equation

$$\dot{Q}_{\text{pb}} = \lambda_{\text{pb}} Q_{\text{Rn}} - \lambda_{\text{pb}} Q_{\text{pb}} - A_{\text{E}} \mathcal{F} \quad (4)$$

(c.f. equation (1)) where P is the mean ^{210}Pb fallout rate from the atmosphere and A_{E} the area of the Earth's surface over which it is distributed. These equations exclude any supported ^{210}Pb , normally a small fraction, present on atmospheric dust particles. ^{210}Pb dating is concerned only with the unsupported component.

It is reasonable to suppose that on timescales of a year or more the global inventories are in a state of near equilibrium, that is, $\dot{Q}_{\text{Rn}} = \dot{Q}_{\text{pb}} = 0$. Assuming further that the mean ^{210}Pb fallout rate is proportional to the global ^{210}Pb inventory we can write

$$A_{\text{E}} \mathcal{F} = k_{\text{g}} Q_{\text{pb}} \quad (5)$$

where k_{g} is a mean global loss-rate coefficient. It then follows that the global ^{222}Rn inventory can be written

$$Q_{\text{Rn}} = \frac{A_{\text{L}} \mathcal{F}}{\lambda_{\text{Rn}}}$$

and the mean ^{210}Pb fallout rate

$$P = \frac{k_{\text{g}}}{\lambda_{\text{pb}} + k_{\text{g}}} \frac{\lambda_{\text{pb}}}{\lambda_{\text{Rn}}} \frac{A_{\text{L}}}{A_{\text{E}}} \mathcal{F}.$$

Estimates of the ^{210}Pb atmospheric residence time suggest that it is measured in days or at most weeks, and so is negligible compared to the radioactive ^{210}Pb half-life (22.26 years). The radioactive decay constant λ_{pb} will accordingly be negligible compared to the loss rate k_{g} . It follows that to a close approximation the above equation can be written

$$P = \frac{\lambda_{\text{pb}}}{\lambda_{\text{Rn}}} \frac{A_{\text{L}}}{A_{\text{E}}} \mathcal{F}. \quad (6)$$

If the ^{222}Rn emanation rate and decay constant are measured in $\text{Bq m}^{-2} \text{d}^{-1}$ and d^{-1} and the ^{210}Pb decay constant measured in y^{-1} , from dimensional arguments this equation will give the ^{210}Pb flux in $\text{Bq m}^{-2} \text{y}^{-1}$.

Although applicable to the atmosphere as a whole, since there is relatively little exchange between the Northern and Southern Hemispheres these equations are to a good approximation also applicable to the two hemispheres separately. Whereas inter-hemispheric exchanges take place on timescales of a few years (Junge, 1962), the atmospheric residence times of these radionuclides are measured in days or weeks. Estimates of the mean ^{222}Rn exhalation rate from land surfaces vary from $\sim 0.7 \text{ atom cm}^{-2} \text{ s}^{-1}$ (Israël, 1951) to $\sim 1.2 \text{ atom cm}^{-2} \text{ s}^{-1}$ (Turekian et al., 1977). Although the rate will be highly variable on small spatio-temporal scales, it is reasonable to suppose that mean values on longer time-scales of a

year or more will be relatively constant (c.f. Feichter et al., 1991; Liu et al., 2001). Here we assume a value of $1570 \text{ Bq m}^{-2} \text{ d}^{-1}$ ($0.87 \text{ atom cm}^{-2} \text{ s}^{-1}$) determined from the atmospheric inventories at continental sites where the vertical distribution is close to the equilibrium state (Piliposian and Appleby, 2003). This approach does in principle integrate inputs from all sources over large geographical areas. Global balances have been calculated by applying the above figure to the c.74% of Earth's continental land surface free of ice sheets, permafrost and fresh water bodies ($\sim 1.1 \times 10^8 \text{ km}^2$). We have also assumed an exhalation rate of $\sim 10 \text{ Bq m}^{-2} \text{ d}^{-1}$ (Wilkening and Clements, 1975) from the oceans ($\sim 3.62 \times 10^8 \text{ km}^2$). Given that $\sim 70\%$ of the ice-free land is in the Northern Hemisphere, the mean ^{210}Pb flux from the atmosphere is calculated to be $\sim 80 \text{ Bq m}^{-2} \text{ y}^{-1}$ in the Northern Hemisphere and $\sim 38 \text{ Bq m}^{-2} \text{ y}^{-1}$ in the Southern Hemisphere. Considering the fact that information on ^{210}Pb fallout over much of the Earth's surface (and particularly the oceans) is very sparse, these figures are relatively consistent with values determined from the Liverpool University ERRC (Environmental Radioactivity Research Centre) global database on ^{210}Pb fallout. The ERRC holds one of the world's most comprehensive collection of ^{210}Pb fallout data, accumulated over a period of more than 30 years as part of the program of ^{210}Pb dating. These data suggest a mean ^{210}Pb flux of $\sim 73 \text{ Bq m}^{-2} \text{ y}^{-1}$ in the Northern Hemisphere and $\sim 39 \text{ Bq m}^{-2} \text{ y}^{-1}$ in the Southern Hemisphere (Appleby and Piliposian, 2010).

Data from sites in continental USA, Europe and Asia lying within the largely ice-free northern mid-latitudes (30° – 65°N) suggest that the ^{222}Rn – ^{210}Pb cycle (measured on long time-scales) is largely self-contained in this zone. Since dry land occupies around 51% of this total area it follows from equation (6) that ^{222}Rn exhalation would if contained generate a mean ^{210}Pb flux of $139 \text{ Bq m}^{-2} \text{ y}^{-1}$. The mean empirical value from our database is $\sim 136 \text{ Bq m}^{-2} \text{ y}^{-1}$. Given that intrahemispheric mixing is thought to take place on timescales of a few months (Warneck, 2000), this approximate balance (though once again keeping in mind the sparsity of the data) is again consistent with the notion that ^{210}Pb has a relatively short tropospheric residence time. The distribution of fallout within this zone is however strongly influenced by the major continental land masses. Driven by the predominantly west-to-east global circulation, air masses arriving at the western margins of North America and Eurasia are depleted in ^{222}Rn and ^{210}Pb during their passage over the Pacific and Atlantic oceans but replenished by ^{222}Rn exhalation during their passage over the land masses. This is demonstrated by the regional data on mean annual fallout of ^{210}Pb in North America and Eurasia shown in Fig. 1. Fallout data from the Liverpool University ERRC database (encompassing data from around 250 sites) has been grouped together on a regional basis and mean values calculated for each region. ^{210}Pb fallout has its highest values near the eastern margins of the continental land masses where the flux can exceed $200 \text{ Bq m}^{-2} \text{ y}^{-1}$ (per meter of

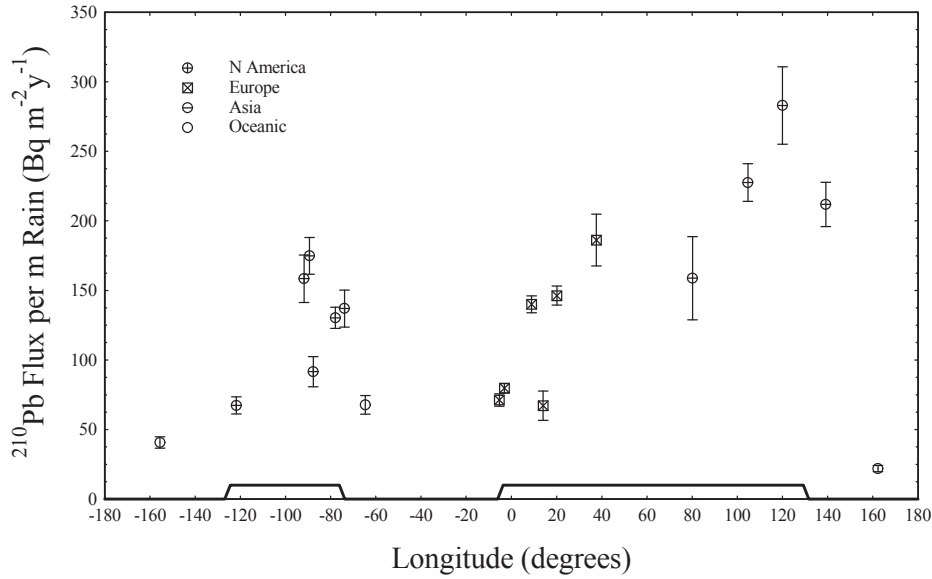


Fig. 1. Mean annual fallout of ^{210}Pb (normalised against rain) at sites in North America and Eurasia extracted from the Liverpool University ERRC global database. Each point represents the average value for all fallout data within a given geographical region.

rainfall).

A similar distribution was obtained theoretically by Turekian et al. (1977) by applying mass balance principles to a notional vertical column of air moving over the Earth's surface at northern mid latitudes. The model assumed a predominately west-to-east global circulation, a steady circulation velocity, a uniform ^{222}Rn exhalation rate from land surfaces and negligible emissions from the oceans. It also assumed a mean ^{210}Pb residence time of 5 days. Writing Q_{Rn} and Q_{Pb} for the radionuclide inventories of the column per unit area the calculations in effect solved equations (3)–(5) to determine variations in the ^{210}Pb flux P with longitude.

2.2. Transport processes within the air column

A major limitation of mass balance models is that they give no information about the vertical distribution of the radionuclides within the column. Nor do they take into account the reservoir effect of the stratosphere. The fallout equation (5) is only applicable to that component of the ^{210}Pb distribution lying within the troposphere. A significant stratospheric component built up during passage over major land masses is slowly released to the troposphere as the air column moves out over large water bodies and the troposphere becomes depleted by fallout. The principal mechanism controlling the vertical distribution of ^{222}Rn and its daughters within an air column will be turbulent diffusion (Jacobi and André, 1963). Since ^{222}Rn (half-life 3.825 days) is an inert gas it is removed from the column only by radioactive decay. Assuming a Lagrangian coordinate system imbedded in the column, its distribution will thus satisfy the partial differential equation

$$\frac{\partial C_{\text{Rn}}}{\partial t} = \frac{\partial}{\partial z} \left(D \frac{\partial C_{\text{Rn}}}{\partial z} \right) - \lambda_{\text{Rn}} C_{\text{Rn}} \quad (7)$$

where $C_{\text{Rn}}(z,t)$ denotes the ^{222}Rn concentration (in Bq m^{-3}) at altitude z and time t , D is an effective vertical diffusivity, and λ_{Rn} is the ^{222}Rn radioactive decay constant. The boundary conditions are

$$-D \frac{\partial C_{\text{Rn}}}{\partial z} \Big|_{(0,t)} = F, \quad C_{\text{Rn}}(z,t) \rightarrow 0 \text{ as } z \rightarrow \infty \quad (8)$$

where F denotes the ^{222}Rn flux (in Bq m^{-2}) by emanation from the Earth's surface into the base of the column. In contrast to ^{222}Rn , ^{210}Pb atoms are highly reactive and readily adsorbed onto dust particles, and may be removed from the atmosphere by wet and dry deposition, as well as by radioactive decay to its daughter radionuclides ^{210}Bi (half-life 5.013 d) and ^{210}Po (half-life 138.4 d). Adding terms for this process, the ^{210}Pb concentration $C_{\text{Pb}}(z,t)$ (in Bq m^{-3}) will be governed by the partial differential equation

$$\frac{\partial C_{\text{Pb}}}{\partial t} = \frac{\partial}{\partial z} \left(D \frac{\partial C_{\text{Pb}}}{\partial z} \right) + \lambda_{\text{Pb}} (C_{\text{Rn}} - C_{\text{Pb}}) - \Lambda(C_{\text{Pb}}) \quad (9)$$

and boundary conditions

$$\frac{\partial C_{\text{Pb}}}{\partial z} \Big|_{(0,t)} = 0, \quad C_{\text{Pb}}(z,t) \rightarrow 0 \text{ as } z \rightarrow \infty \quad (10)$$

where $\Lambda(C_{\text{Pb}})$ is a term characterizing the rate at which ^{210}Pb condenses from the aerosol state dominated by turbulent diffusion to incipient precipitation dominated by gravity. In Piliposian and Appleby (2003) equations (7)–(10) were solved numerically, assuming a constant diffusivity $D = 2.7 \text{ km}^2 \text{ d}^{-1}$ ($3.1 \times 10^5 \text{ cm}^2 \text{ s}^{-1}$) and a mean ^{222}Rn flux from land surfaces of $1570 \text{ Bq m}^{-2} \text{ d}^{-1}$. The values of these parameters were determined from vertical ^{222}Rn distributions at sites where this radionuclide appeared to have reached equilibrium. The fact that the mean empirical profiles at these sites could be represented by an exponential relation suggests that the assumption of a constant diffusivity is a reasonable first approximation. We follow Piliposian and Appleby (2003) in supposing that droplet formation occurs only in the troposphere. The value of the term $\Lambda(C_{\text{Pb}})$ characterizing the rate at which ^{210}Pb condenses from the aerosol state is thus effectively zero in the stratosphere. Its value in the troposphere was assumed to be proportional to the ^{210}Pb concentration and so could be written

$$A(C_{Pb}) = \kappa C_{Pb} \{1 - H(z - z_1)\}$$

where κ is a tropospheric removal rate constant, $H(z)$ the Heaviside function defined by

$$H(z) = \begin{cases} 0 & z \leq 0 \\ 1 & z > 0 \end{cases},$$

and z_1 the height of the tropopause. The reciprocal of κ is a measure of the tropospheric residence time. It is again important to emphasise that these equations and concepts are only meaningful when applied to quantities time-averaged over sufficiently long time-scales to smooth out short-term fluctuations. For numerical calculations it was more practical, both from a mathematical and physical point of view, to replace the Heaviside function by the differentiable function

$$\frac{1}{2}(1 + \tanh(\beta z)),$$

whence

$$\Lambda(C_{Pb}) = \kappa C_{Pb} \left\{ \frac{1}{2}(1 - \tanh(\beta z)) \right\}.$$

This will give a transition zone at the tropopause of thickness δ across which the value of the term

$$\frac{1}{2}(1 - \tanh(\beta z))$$

in the condensation function declines from 0.95 to 0.05 provided β is chosen so that $\beta > 3/\delta$.

The transport processes for ^{210}Bi and ^{210}Po can reasonably be presumed to follow those of ^{210}Pb . Much of their production will take place after ^{210}Pb atoms have become attached to dust or aerosol particles. The atmospheric concentrations of ^{210}Bi and ^{210}Po (in Bq m^{-3}) can thus be assumed to satisfy the partial differential equations

$$\frac{\partial C_{Bi}}{\partial t} = \frac{\partial}{\partial z} \left(D \frac{\partial C_{Bi}}{\partial z} \right) + \lambda_{Bi}(C_{Bi} - C_{Pb}) - \Lambda(C_{Bi}) \tag{11}$$

$$\frac{\partial C_{Po}}{\partial t} = \frac{\partial}{\partial z} \left(D \frac{\partial C_{Po}}{\partial z} \right) + \lambda_{Po}(C_{Po} - C_{Bi}) - \Lambda(C_{Po}) \tag{12}$$

together with the boundary conditions

$$\left. \frac{\partial C_{Bi}}{\partial z} \right|_{(0,t)} = 0, \quad C_{Bi}(z, t) \rightarrow 0 \text{ as } z \rightarrow \infty, \tag{13}$$

$$\left. \frac{\partial C_{Po}}{\partial z} \right|_{(0,t)} = 0, \quad C_{Po}(z, t) \rightarrow 0 \text{ as } z \rightarrow \infty. \tag{14}$$

Here we solve these equations numerically and use the results to calculate the distributions of the isotope ratios $^{210}\text{Bi}/^{210}\text{Pb}$ and $^{210}\text{Po}/^{210}\text{Pb}$ for different values of the tropospheric removal rate constant κ . The results are compared with the available empirical data in order to determine the extent to which these data can be used to provide a good estimate of the tropospheric residence time.

3. Numerical approach

The value of the ^{222}Rn flux F in the boundary condition (8) for equation (7) will depend mainly on whether the column is moving

over land or water. Exhalation rates from oceans are estimated to be two orders of magnitude less than those from ice-free land surfaces. Although the distributions of ^{222}Rn and its daughter radionuclides ^{210}Pb , ^{210}Bi and ^{210}Po for the case of a prolonged ^{222}Rn flux F into the base of the column can be obtained by using the MATHEMATICA software to solve *ab initio* the system of partial differential equations and boundary conditions (7)–(14), a numerically more stable solution is obtained by using a Green's function approach, whereby we first consider the response of the system to a brief impulsive input of ^{222}Rn

$$\mathcal{F}(t) = I_0 \delta(t) \tag{15}$$

where $\delta(t)$ is the Dirac delta function. The response to a prolonged ^{222}Rn input can then be constructed by representing it as a series of discrete inputs and superimposing the responses to different inputs at different times.

Under conditions of a constant diffusivity the ^{222}Rn distribution for a brief impulsive input has the exact analytical solution

$$C_{Rn}(z, t) = I_0 e^{-\lambda_{Rn}t} \frac{1}{\sqrt{\pi Dt}} e^{-\frac{z^2}{4Dt}} = I_0 G_{Rn}(z, t) \tag{16}$$

where

$$G_{Rn}(z, t) = \frac{e^{-\lambda_{Rn}t}}{\sqrt{\pi Dt}} e^{-\frac{z^2}{4Dt}} \tag{17}$$

is the response to a unit input at time $t = 0$ (Piliposian & Appleby, 2003). Substituting this function into equation (9) the three partial differential equations for ^{210}Pb , ^{210}Bi and ^{210}Po were solved in turn numerically to give three Green's functions

$$G_{Pb}(z, t), \quad G_{Bi}(z, t), \quad G_{Po}(z, t) \tag{18}$$

characterising the further responses of the system to an impulsive ^{222}Rn input. Numerical calculations of these functions have been carried out for values of the tropospheric removal rate constant κ ranging from 0.08 d^{-1} (12.5 days residence time) to 0.3 d^{-1} (3.3 days residence time).

For a prolonged ^{222}Rn flux $F(s)$ ($0 < s < t$), noting that the contribution of the amount of ^{222}Rn injected into the atmosphere at time τ during the time interval $d\tau$ to the ^{222}Rn distribution at time t will be

$$G_{Rn}(z, t - \tau) \mathcal{F}(\tau) d\tau = G_{Rn}(z, s) \mathcal{F}(t - s) ds \quad \text{where } s = t - \tau$$

the ^{222}Rn distribution has an exact analytical form

$$C_{Rn}(z, t) = \int_0^t \frac{e^{-\lambda_{Rn}s}}{\sqrt{\pi Ds}} e^{-\frac{z^2}{4Ds}} \mathcal{F}(t - s) ds = \int_0^t G_{Rn}(z, s) \mathcal{F}(t - s) ds \tag{19}$$

The distributions of the daughter radionuclides can similarly be written

$$\left. \begin{aligned} C_{Pb}(z, t) &= \int_0^t G_{Pb}(z, s) \mathcal{F}(t-s) ds \\ C_{Bi}(z, t) &= \int_0^t G_{Bi}(z, s) \mathcal{F}(t-s) ds \\ C_{Po}(z, t) &= \int_0^t G_{Po}(z, s) \mathcal{F}(t-s) ds \end{aligned} \right\} \quad (20)$$

though these must be determined numerically. The procedure used for carrying out these calculations is given in the Appendix A. The validity of the solutions has been checked very carefully using mass balance arguments, by comparison with the equilibrium ²²²Rn distribution for a constant ²²²Rn flux over a long period of time, and also by comparison with standard numerical solutions of the governing equations using MATHEMATICA. Although the two methods were in good agreement over short to medium time-scales, the Green's function method was numerically much more stable over long time-scales, where ²²²Rn concentrations had decayed to very low values.

4. Global equilibrium distribution for northern mid-latitudes

The above approach is used here to model the mean annual distribution of the ²²²Rn daughters ²¹⁰Pb, ²¹⁰Bi, and ²¹⁰Po in the atmosphere at northern mid-latitudes. The results are fitted to the available empirical data in order to determine a best value for the removal rate constant κ . From a model validation point of view these regions, defined as 30°–65°N spanning continental USA and Western Europe as far north as central Scandinavia (Fig. 2), have the advantage of a relatively good coverage of data on the distribution and fallout of ²¹⁰Pb (Fig. 1). They also cover virtually all the available empirical data on the daughter products ²¹⁰Bi and ²¹⁰Po (Table 1).

Although ²²²Rn exhalation rates from land surfaces are subject to short-term seasonal and weather-related fluctuations, mean annual inputs to the atmosphere will be relatively constant on longer timescales of a year or more. On these timescales the mean annual spatial distributions of the ²²²Rn daughters ²¹⁰Pb, ²¹⁰Bi, and ²¹⁰Po will also be similar from year to year. The distribution within a notional column moving from west to east may thus be assumed to be a periodic function of longitude θ (period 360°), or equivalently, of the time t with a period equal to the global transit time T . Using

estimates from a range of different sources, Piliposian and Appleby (2003) estimated the mean annual global transit time to be around 78 days. Since the largely ice-free land within these northern mid-latitudes occupies roughly 51% of the total area, on each circuit and the column would spend 40 days over land and 38 days over the ocean. To a reasonable approximation, this can be divided into 11 days over North America, 16 days over the Atlantic, 29 days over Eurasia, and 22 days over the Pacific. Assuming a ²²²Rn exhalation rate over land of $F = 1570 \text{ Bq m}^{-2} \text{ d}^{-1}$, and negligible inputs from the oceans, the ²²²Rn exhalation rate into the base of the column will be

$$\mathcal{F}(t) = \mathcal{F}\{H(t-t_0) - H(t-t_1) + H(t-t_2) - H(t-t_3)\} \quad (21)$$

where t_0 is the time at which the column crosses the western seaboard of North America, t_1 the time at which it crosses the eastern seaboard, t_2 the time at which it crosses the western seaboard of Europe, and t_3 the time at which it crosses the eastern margin of the Eurasian land mass. For numerical calculations the Heaviside function $H(t)$ can be approximated by the differentiable function

$$\frac{1}{2}(1 + \tanh(\alpha t))$$

where the value of the parameter α is chosen so as to give suitably small transition zones across seaboards.

4.1. Equilibrium Green's functions

Solving the governing partial differential equations (7)–(14) starting from a zero initial condition, in order to determine the equilibrium (periodic) distribution it would be necessary to track the solution over several circuits of the globe. This approach can however result in the build up of significant numerical errors. The process can be simplified, and made more accurate by introducing the notion of an equilibrium Green's function.

Each time the column passes a fixed point on the Earth's surface it will receive a brief impulsive input of ²²²Rn from that point the strength of which we denote by I_0 . Setting the time $t = 0$ just as the column passes this point, the distribution of ²²²Rn in the column at times $t > 0$ due to the input from this location at time $t = 0$ will be $I_0 G_{Rn}(z, t)$ (equation (16)). The distribution at time t due to the input from the same location on the previous circuit (at time $-T$) will be $I_0 G_{Rn}(z, t + T)$. Adding the contributions from inputs on all previous occasions (at times $-kT, k = 0, 1, 2, \dots$), the distribution in the column at times $0 < t < T$ due to present and past inputs from this location will be

$$\begin{aligned} I_0 \{G_{Rn}(z, t) + G_{Rn}(z, t + T) + G_{Rn}(z, t + 2T) + \dots \} \\ = I_0 G_{Rn}^{equ}(z, t) \end{aligned} \quad (22)$$

where

$$G_{Rn}^{equ}(z, t) = \sum_{k=0}^{\infty} G_{Rn}(z, t + kT) \quad (23)$$

represents an equilibrium Green's function for the ²²²Rn distribution. Since the distribution at time $t + T$ will be the same as the distribution at time t , this function will be a periodic function of period T .

The solutions for the ²²²Rn daughters due to this impulse can be similarly written as periodic functions

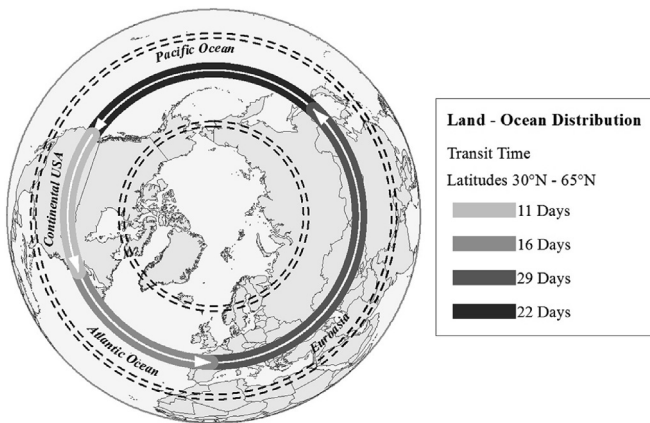


Fig. 2. Map of the Earth's northern hemisphere showing the land lying between 30°–65°N. Also shown are the approximate transit times across the major land masses and oceans for a notional air column moving from west to east.

$$\left. \begin{aligned} I_0 G_{Pb}^{equ}(z, t) &= I_0 \sum_{k=0}^{\infty} G_{Pb}(z, t + kT) \\ I_0 G_{Bi}^{equ}(z, t) &= I_0 \sum_{k=0}^{\infty} G_{Bi}(z, t + kT) \\ I_0 G_{Po}^{equ}(z, t) &= I_0 \sum_{k=0}^{\infty} G_{Po}(z, t + kT) \end{aligned} \right\} \quad (24)$$

where $G_{Pb}(z, t)$, $G_{Bi}(z, t)$, $G_{Po}(z, t)$ are the corresponding Green's functions for a single impulsive input. The equilibrium Green's functions $G_{Pb}^{equ}(z, t)$, $G_{Bi}^{equ}(z, t)$, $G_{Po}^{equ}(z, t)$ are easily generated by continuing to add terms from previous circuits, up until the values are negligible. In practice we found that 6 periods were sufficient for the longer-lived ^{222}Rn daughters, although because of its short half-life, one period (78 days) was sufficient for ^{222}Rn itself.

Using this concept, the contribution to the equilibrium of ^{222}Rn distribution at longitude θ due to ^{222}Rn emissions from the Earth's surface lying between longitudes ϕ and $\phi - \delta\phi$ will be

$$G_{Rn}^{equ}(z, s) \cdot \mathcal{F}(\phi) \delta s$$

where $\mathcal{F}(\phi)$ is the ^{222}Rn exhalation rate at longitude ϕ , s is the travel-time in a west-to-east direction to reach longitude θ , and δs is the time taken for the column to traverse the incremental longitude $\delta\phi$. If $V (= 360^\circ/T)$ is the circulation velocity, so that $\phi = \theta - Vs$ and $\delta s = \delta\phi/V$, the equilibrium ^{222}Rn distribution at longitude θ will include all such contributions, and will thus be

$$G_{Rn}^{equ}(z, \theta) = \int_0^T G_{Rn}^{equ}(z, s) \cdot \mathcal{F}(\theta - Vs) ds. \quad (25)$$

The equilibrium distributions of the daughter radionuclides can similarly be written

$$\left. \begin{aligned} C_{Pb}(z, t) &= \int_0^t G_{Pb}^{equ}(z, s) \cdot \mathcal{F}(\theta - Vs) ds \\ C_{Bi}(z, t) &= \int_0^t G_{Bi}^{equ}(z, s) \cdot \mathcal{F}(\theta - Vs) ds \\ C_{Po}(z, t) &= \int_0^t G_{Po}^{equ}(z, s) \cdot \mathcal{F}(\theta - Vs) ds \end{aligned} \right\} \quad (26)$$

The numerical procedure for carrying out these calculations is given in [Appendix A](#).

5. Results

5.1. $^{210}\text{Bi}/^{210}\text{Pb}$ and $^{210}\text{Po}/^{210}\text{Pb}$ concentration ratios in ground-level air

Fig. 3 plots modelled values of the $^{210}\text{Bi}/^{210}\text{Pb}$ and $^{210}\text{Po}/^{210}\text{Pb}$ concentration ratios in ground-level air at mid-latitudes as functions of longitude θ for values of the tropospheric removal rate constant κ ranging from 0.08 d^{-1} to 0.2 d^{-1} calculated using equation (26). Also shown are mean empirical values calculated from all the measurements of ^{210}Pb , ^{210}Bi and ^{210}Po in ground level air carried out at sites in Colorado ($\sim 105^\circ\text{W}$, [Poet et al., 1972](#)), Lisbon Portugal ($\sim 9^\circ\text{W}$, [Carvalho, 1995](#)) and Hawaii ($\sim 156^\circ\text{W}$, [Moore et al., 1974](#)) and from ^{210}Pb and ^{210}Po measurements at Harwell UK ($\sim 1^\circ\text{W}$, [Burton and Stewart, 1960](#); [Peirson et al., 1966](#)).

It is evident from these results that for any given value of κ the

theoretical $^{210}\text{Bi}/^{210}\text{Pb}$ and $^{210}\text{Po}/^{210}\text{Pb}$ concentration ratios vary considerably, the variations largely being governed by the position of the air column relative to major land masses. The $^{210}\text{Bi}/^{210}\text{Pb}$ ratio increases rapidly over large oceans to values close to unity (radioactive equilibrium). Renewed ^{210}Pb production at the western margins of the major land masses causes its value to fall dramatically, reaching a minimum value after approximately 4 days in the case of $\kappa = 0.2$ (minimum value 0.23) or 7 days in the case of $\kappa = 0.08$ (minimum value 0.43). As the column moves further into the land mass, increased ^{210}Bi production results in a gradual increase in the $^{210}\text{Bi}/^{210}\text{Pb}$ ratio. Reduced ^{210}Pb production once the column has crossed the eastern seaboard and moves out over the ocean causes a sharp acceleration in the rate of increase. The $^{210}\text{Po}/^{210}\text{Pb}$ ratios follow a similar pattern though values are an order of magnitude lower due to the longer ^{210}Po half-life.

Empirical values of the raw $^{210}\text{Bi}/^{210}\text{Pb}$ concentration ratio in surface air at the Colorado site ranged from 0.18 to 0.65 with a mean value of 0.41 ± 0.02 . Those at Lisbon ranged from 0.12 to 1.33 with a mean value of 0.57 ± 0.10 , whilst those at Hawaii at sea level on the windward side of the island ranged from 0.81 to 0.97 with a mean value of 0.84 ± 0.03 . The results from the Colorado and Hawaiian sites suggest that the value of κ lies between 0.08 and 0.1. Although measured results from Lisbon suggest a higher value of κ , its position on the western edge of Europe where values of the $^{210}\text{Bi}/^{210}\text{Pb}$ concentration ratio change rapidly with distance makes the use of data from this location highly problematic. Further, the mean value may well be significantly influenced by local prevailing factors. $^{210}\text{Bi}/^{210}\text{Pb}$ values at this site determined during times of westerly air flows will have much higher values than those determined during times of easterly conditions.

$^{210}\text{Po}/^{210}\text{Pb}$ ratios are an order of magnitude lower than the $^{210}\text{Bi}/^{210}\text{Pb}$ ratios. Raw values at ground-level at the Colorado site ranged from 0.03 to 0.25 with a mean value of 0.082 ± 0.012 . Those at Lisbon ranged from 0.03 to 0.78 with a mean value of 0.17 ± 0.05 . The mean value at Harwell, also a problematic location, was 0.16 ± 0.05 . At Hawaii the $^{210}\text{Po}/^{210}\text{Pb}$ ratio at sea level on the windward side of the island ranged from 0.08 to 0.18 with a mean value of 0.10 ± 0.01 . Although these results appear to suggest a significantly lower value of κ , the most likely explanation for the discrepancy would appear to be contamination of samples by ground-level dust containing supported ^{210}Pb and its daughters in radioactive equilibrium ([Poet et al., 1972](#); [Baskaran, 2011](#)). Writing $p = ^{226}\text{Ra}/^{210}\text{Pb}$ for the supported ^{210}Pb fraction the unsupported activities will be $(1 - p)^{210}\text{Pb}$, $^{210}\text{Bi} - p^{210}\text{Pb}$, $^{210}\text{Po} - p^{210}\text{Pb}$. The amount of supported activity can then be estimated by adjusting the value of p so that the unsupported $^{210}\text{Bi}/^{210}\text{Pb}$ and $^{210}\text{Po}/^{210}\text{Pb}$ activity ratios yield the same value of κ . The results of these calculations, shown in [Table 2](#), suggest a relatively low amount of supported ^{210}Pb , varying from 3.4% to 5.3% of the total ^{210}Pb activity. Because of the low ^{210}Po activities this correction has a disproportionate effect on the $^{210}\text{Po}/^{210}\text{Pb}$ ratio, as shown in [Fig. 3](#). The effect on the much higher $^{210}\text{Bi}/^{210}\text{Pb}$ ratio was relatively insignificant. Excluding the data from the West-European seaboard (Lisbon and Harwell) the value of κ was calculated to be between $0.09 \pm 0.02 \text{ d}^{-1}$ (Hawaiian data) and $0.11 \pm 0.01 \text{ d}^{-1}$ (Colorado data).

5.2. $^{210}\text{Bi}/^{210}\text{Pb}$ and $^{210}\text{Po}/^{210}\text{Pb}$ tropospheric inventory ratios

Fig. 4 shows modelled values of the $^{210}\text{Bi}/^{210}\text{Pb}$ and $^{210}\text{Po}/^{210}\text{Pb}$ tropospheric inventory ratios calculated for values of the tropospheric removal rate constant κ ranging from 0.08 d^{-1} to 0.2 d^{-1} . The results follow a similar pattern to those for ground-level air. $^{210}\text{Bi}/^{210}\text{Pb}$ ratios increase rapidly over large oceans to values close to radioactive equilibrium, but then fall steeply as the column arrives at the western margins of the major land masses. Minimum

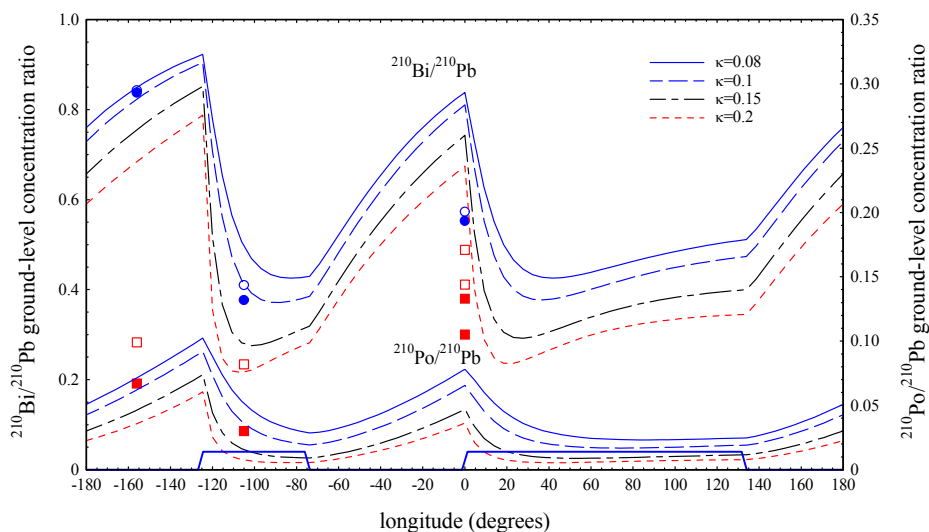


Fig. 3. Modelled values of the $^{210}\text{Bi}/^{210}\text{Pb}$ (left-hand axis) and $^{210}\text{Po}/^{210}\text{Pb}$ (right-hand axis) activity ratios in ground-level air at northern mid-latitudes plotted versus longitude for values of the tropospheric removal rate constant ranging from 0.08 d^{-1} to 0.2 d^{-1} , showing also the major land masses. Mean activity ratios for Hawaii, the interior of the USA, and the western margin of Europe calculated from all the available empirical data are shown by the symbols \circ ($^{210}\text{Bi}/^{210}\text{Pb}$) and \square ($^{210}\text{Po}/^{210}\text{Pb}$). Unsupported activity ratios are represented by the solid symbols (\bullet , \blacksquare).

Table 2

Mean values of the empirical ^{210}Pb , ^{210}Bi and ^{210}Po activity ratios, supported ^{210}Pb , corrected (unsupported) activity ratios, and the tropospheric removal rate determined by fitting the empirical data to the modelled values.

Longitude	Raw values		Supported ^{210}Pb	Corrected values		κ d^{-1}
	$^{210}\text{Bi}/^{210}\text{Pb}$	$^{210}\text{Po}/^{210}\text{Pb}$		$^{210}\text{Bi}/^{210}\text{Pb}$	$^{210}\text{Po}/^{210}\text{Pb}$	
<i>(a) Ground-level concentration ratios</i>						
-156	0.84 ± 0.03	0.10 ± 0.01	3.4%	0.84 ± 0.03	0.067	0.09 ± 0.02
-105	0.41 ± 0.02	0.082 ± 0.012	5.3%	0.38 ± 0.02	0.030	0.11 ± 0.01
0	0.57 ± 0.10	0.17 ± 0.05	4.4%	0.55 ± 0.10	0.13	
0		0.16 ± 0.05	4.4%		0.11	
<i>(b) Tropospheric inventories ratios</i>						
-101	0.62 ± 0.04	0.11 ± 0.02	4.4%	0.61 ± 0.04	0.069	0.09 ± 0.01
0		0.10 ± 0.02	4.4%		0.061	
<i>Mean value</i>						0.097 ± 0.012

NB: The standard errors given in this Table are based on the 1σ counting errors reported in the original publications (Table 1).

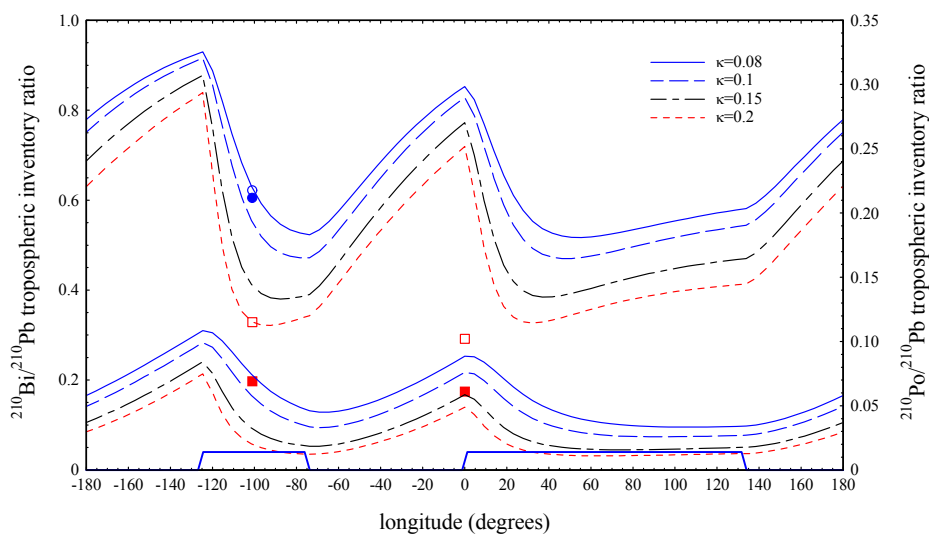


Fig. 4. Modelled values of the $^{210}\text{Bi}/^{210}\text{Pb}$ (left-hand axis) and $^{210}\text{Po}/^{210}\text{Pb}$ (right-hand axis) tropospheric inventory ratios at northern mid-latitudes plotted versus longitude. Values of the tropospheric removal rate constant range from 0.08 d^{-1} to 0.3 d^{-1} , also showing the major land masses. Mean activity ratios for the interior of the USA and the western margin of Europe, calculated from all the available empirical data, are shown by the symbols \circ ($^{210}\text{Bi}/^{210}\text{Pb}$) and \square ($^{210}\text{Po}/^{210}\text{Pb}$). Unsupported activity ratios are represented by the solid symbols (\bullet , \blacksquare).

values over the land masses are reached after around 6 days in the case $\kappa = 0.2 \text{ d}^{-1}$ (minimum value 0.32) or 10 days in the case $\kappa = 0.08 \text{ d}^{-1}$ (minimum value 0.53). $^{210}\text{Po}/^{210}\text{Pb}$ ratios are again an order of magnitude lower than the $^{210}\text{Bi}/^{210}\text{Pb}$ ratios.

Since the isotopic composition of the troposphere as a whole is likely to be reflected in the isotopic composition of rainwater, empirical measurements of the $^{210}\text{Bi}/^{210}\text{Pb}$ and $^{210}\text{Po}/^{210}\text{Pb}$ tropospheric inventory ratios are most readily made using rainwater samples. Measurements of ^{210}Pb , ^{210}Bi and ^{210}Po in rainwater were carried out at sites in Colorado ($\sim 105^\circ\text{W}$, Poet et al., 1972) and Arkansas (94°W , Gavini et al., 1974). Measurements of ^{210}Pb and ^{210}Po in rainwater were carried out at Harwell (Burton and Stewart, 1960). A more direct estimate of tropospheric inventory ratios can be made using measured profiles of ^{210}Pb , ^{210}Bi and ^{210}Po in the atmosphere. Concentrations of these radionuclides at altitudes ranging from ground-level up to 17 km were determined by Moore et al. (1973) at a number of sites in continental USA ranging from Utah ($\sim 112^\circ\text{W}$) to Kansas ($\sim 95^\circ\text{W}$). Many of the measurements were repeated on a number of separate occasions. Tropospheric inventories calculated by combining all the atmospheric profiles yielded a mean $^{210}\text{Bi}/^{210}\text{Pb}$ ratio of 0.52 ± 0.05 . Values calculated from rainwater measurements at the Colorado site ranged from 0.48 to 0.84 with a mean value of 0.61 ± 0.01 . Those from the Arkansas site ranged from 0.32 to 1.05 with a mean value of 0.74 ± 0.10 . Averaging all these results, a best estimate of the mean $^{210}\text{Bi}/^{210}\text{Pb}$ tropospheric inventory ratio for the interior of continental USA is 0.62 ± 0.04 . Similar calculations of the mean $^{210}\text{Po}/^{210}\text{Pb}$ tropospheric inventory ratio for the interior of continental USA yielded values of 0.14 ± 0.03 from the atmospheric profiles, 0.061 ± 0.005 from the Colorado rainwater measurements, and 0.13 ± 0.02 from the Arkansas rainwater measurements, with a mean value of 0.11 ± 0.02 . The Harwell rainwater measurements had a mean $^{210}\text{Po}/^{210}\text{Pb}$ ratio of 0.10 ± 0.02 .

The raw tropospheric $^{210}\text{Bi}/^{210}\text{Pb}$ ratio from the continental USA suggests a value of κ comparable to that determined from the ground-level data. The raw $^{210}\text{Po}/^{210}\text{Pb}$ activity ratio again suggests a much lower value, presumably due to the disproportionate effect of a small amount of supported activity estimated in this case to be just 4.4% of the total ^{210}Pb activity. The corrected unsupported activity ratios are shown in Fig. 4. These results, also given in detail in Table 2, yielded a value of $\kappa = 0.09 \pm 0.01 \text{ d}^{-1}$ similar to that determined from the ground-level data. Averaging the results from both data sets, a best estimate of the tropospheric removal rate constant is $0.097 \pm 0.012 \text{ d}^{-1}$, corresponding to a residence time of 10.3 ± 1.2 days. In practice we round these figures to $\kappa = 0.10 \text{ d}^{-1}$ and the residence time to 10 days.

6. Reservoir effect of the stratosphere

Although the theoretical tropospheric residence time of ^{210}Pb and its daughters appears to be around 10 days, the practical residence time is significantly greater due to the reservoir effect of the stratosphere. ^{222}Rn and its daughters are transported from the troposphere to the stratosphere when concentrations are higher in the troposphere. This process is reversed once tropospheric concentrations fall below those in the stratosphere. Fig. 5 plots the tropospheric, stratospheric and total ^{210}Pb inventories (including fallout) versus time, resulting from an impulsive ground-level ^{222}Rn input of 1570 Bq m^{-2} at time $t = 0$, for the case $\kappa = 0.1$. The inventories were calculated by numerical integration of the ^{210}Pb profiles given by the Green's function $I_0 G_{\text{Pb}}(z, t)$ (equation (18)) with $I_0 = 1570 \text{ Bq m}^{-2}$. The good agreement of the total ^{210}Pb inventory with the theoretical values determined from the mass balance equation

$$A_{\text{Pb}}(t) = I_0 \frac{\lambda_{\text{Pb}}}{\lambda_{\text{Rn}} - \lambda_{\text{Pb}}} \left(e^{-\lambda_{\text{Pb}} t} - e^{-\lambda_{\text{Rn}} t} \right), \quad (27)$$

also plotted in Fig. 5, demonstrates the accuracy of the numerical calculations. According to equation (27) the total ^{210}Pb inventory should reach a maximum value of 0.74 Bq m^{-2} after approximately 40 days, though 90% of this value is achieved after just 24 days. Production by ^{222}Rn is then effectively zero, and thereafter the ^{210}Pb inventory declines slowly in accordance with the ^{210}Pb radioactive decay law.

From the numerical calculations the ^{210}Pb inventory in the troposphere reaches a maximum value of 0.32 Bq m^{-2} after just 6 days. Up to around 40 days it then declines rapidly at a rate corresponding to an apparent residence time of around 13 days due mainly to a combination of reduced creation by ^{222}Rn decay and loss by fallout. After around 22 days the tropospheric inventory falls below that of the stratosphere causing a reverse flux from the stratosphere. This becomes significant after around 60 days, slowing down the rate of decline in the troposphere and increasing the residence time of the remaining tropospheric inventory to around 25 days.

The stratospheric inventory reaches a maximum value of around 0.12 Bq m^{-2} after 19 days, at which point it is almost equal to that in the troposphere. It then begins a long slow decline due to depletion of the ^{222}Rn and the reverse flux to the troposphere. This decline has a residence time of 25 days, similar to that of the tropospheric inventory, transport rates from the stratosphere to the troposphere then matching fallout rates from the troposphere. Fallout from the atmosphere has declined by 50% from its maximum value after around 18 days, 90% after around 40 days, and 99% after around 90 days. Given a mean global circulation velocity of around 360 km d^{-1} (corresponding to the global circulation time of 78 days), these results show that fallout originating in ^{222}Rn inputs from a particular source reaches a maximum value after the column has travelled a distance of $\sim 2000 \text{ km}$. It then falls to around 50% of this value after $\sim 6500 \text{ km}$.

Assuming no stratospheric reservoir effect and that the removal constant κ applies to the atmosphere as a whole, the atmospheric inventory would be given by the equation

$$A_{\text{Pb}}(t) = I_0 \frac{\lambda_{\text{Pb}}}{\lambda_{\text{Rn}} - \lambda_{\text{Pb}} - \kappa} \left(e^{-(\lambda_{\text{Pb}} + \kappa)t} - e^{-\lambda_{\text{Rn}} t} \right) \quad (28)$$

This result, also plotted in Fig. 5, shows that the reservoir effect only becomes significant after around 35 days.

7. Discussion

The results presented in this paper show that while the $^{210}\text{Bi}/^{210}\text{Pb}$ and $^{210}\text{Po}/^{210}\text{Pb}$ activity ratios can potentially provide important information on the ^{210}Pb atmospheric residence time, the sampling location plays an important role that must be taken into account. The $^{210}\text{Bi}/^{210}\text{Pb}$ ratios are probably the more reliable, being less influenced by traces of supported activity. Discrepancies between the $^{210}\text{Bi}/^{210}\text{Pb}$ and $^{210}\text{Po}/^{210}\text{Pb}$ ratios can be used to make small corrections for the supported activity. Although the $^{210}\text{Bi}/^{210}\text{Pb}$ ratios have their highest values in air masses approaching western continental margins, the rapid decline in values (especially at ground-level) as the column moves into the land mass makes the use of such locations highly problematic for model validation. The most suitable locations would appear to be the interiors of large land masses.

The most extensive and reliable ^{210}Pb , ^{210}Bi , ^{210}Po datasets are those obtained from sites in the interior of continental USA. They

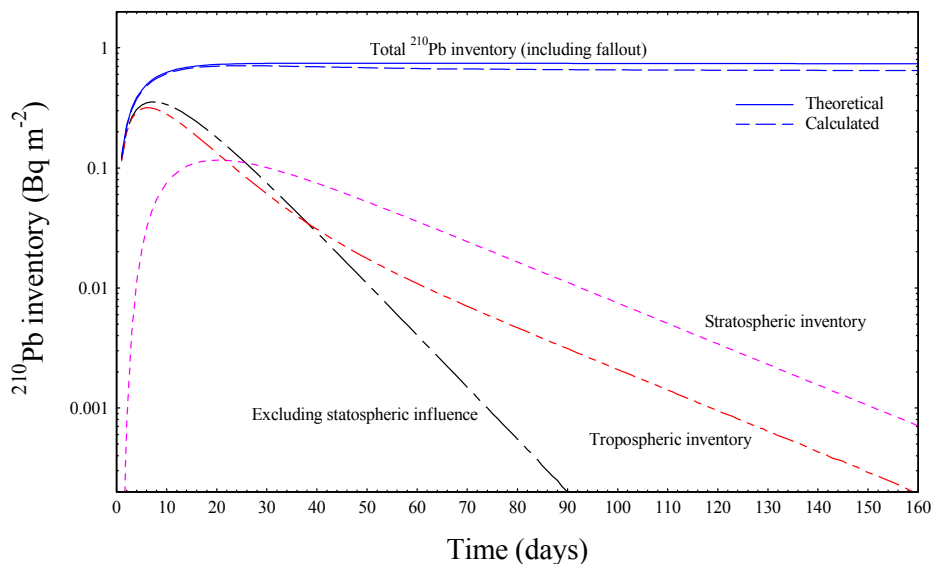


Fig. 5. ^{210}Pb inventories in the troposphere and stratosphere versus time following the brief impulsive injection of 1570 Bq m^{-2} of ^{222}Rn into the base of an air column, calculated from the vertical distribution of the ^{210}Pb activity assuming a tropospheric removal rate coefficient of 0.1 d^{-1} . Also shown are the total ^{210}Pb inventories (including both the atmospheric and fallout components). Values are calculated from both the numerical solutions and the theoretical mass balance equation, assuming no stratospheric reservoir effect to the atmospheric inventory.

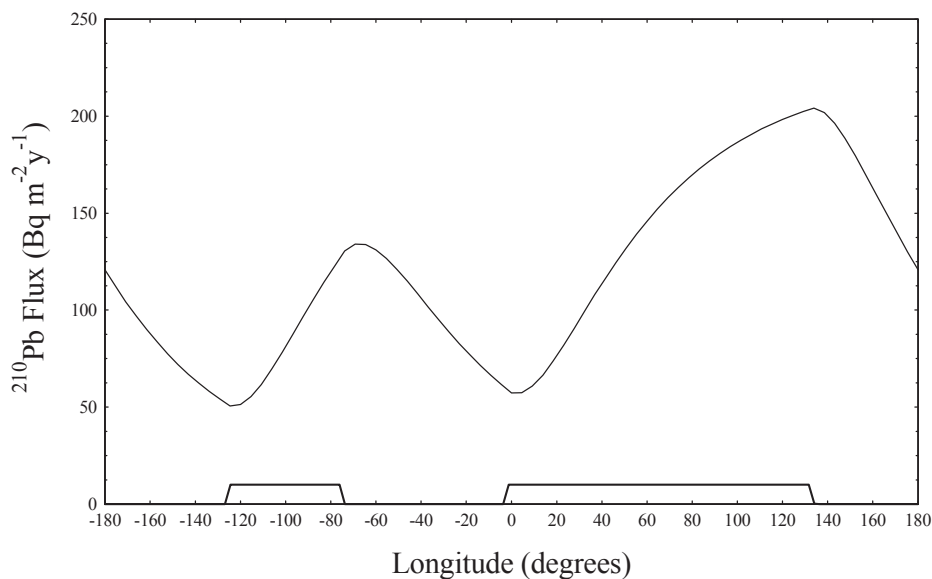


Fig. 6. ^{210}Pb flux at northern mid-latitudes versus longitude assuming a tropospheric removal rate coefficient of 0.1 d^{-1} and global circulation transit time of 78 days.

include measurements carried out on atmospheric samples from a range of different altitudes, and rainwater. Comparisons between the empirical data and model values suggest that the tropospheric removal rate constant has a value between 0.09 and 0.11 d^{-1} . Much higher $^{210}\text{Bi}/^{210}\text{Pb}$ ratios from the oceanic site were also consistent with the model predictions. The corresponding mean tropospheric residence time of 10 days is significantly longer than the value of between 4 and 7 days suggested by Poet et al. (1972) and less than 7 days suggested by Moore et al. (1973). These values were however based on the assumption that ^{222}Rn and its daughters were locally in a state of radioactive equilibrium, governed by equation (1). It is also significantly longer than the value suggested by Piliposian and Appleby (2003) though that was largely based on a review of earlier estimates.

The results presented here also highlight the role played by the

stratosphere in extending the practical residence time of ^{210}Pb in the atmosphere. The reservoir effect of the stratosphere, capturing ^{210}Pb when tropospheric concentrations are high and releasing it when they are low, significantly enhances the long range transport of ^{210}Pb from its source locations. Fig. 6 plots the modelled ^{210}Pb flux versus longitude at northern mid-latitudes assuming a tropospheric removal rate of 0.1 d^{-1} and a 78 day global transit time. The relatively high fluxes at the western margins of Europe and the USA are largely due to long range transport across the Atlantic and Pacific oceans respectively. The model values for these western margins ($\sim 60 \text{ Bq m}^{-2} \text{ y}^{-1}$ for Europe and $\sim 55 \text{ Bq m}^{-2} \text{ y}^{-1}$ for the USA) are comparable to the empirical values for southern England reported by Burton and Stewart (1960) and Peirson et al. (1966), and for coastal regions of western USA reported by Monaghan (1989). Atmospheric fluxes at specific localities within a given region will

however be strongly influenced by local factors such as the mean annual rainfall.

Author contributions

The manuscript was written through contributions from all authors. All authors have given approval to the final version of the manuscript. All authors contributed equally.

Appendix B. Supplementary data

Supplementary data related to this article can be found at <http://dx.doi.org/10.1016/j.jenvrad.2016.04.019>.

Appendix A. Numerical algorithms

Calculation of the radionuclide distributions for a prolonged ²²²Rn flux

In the case of a prolonged ²²²Rn flux $\mathcal{F}(t)$ into the base of the column, assuming a constant diffusivity the distributions of ²²²Rn and its daughter radionuclides ²¹⁰Pb, ²¹⁰Bi, ²¹⁰Po, are given in terms of their respective Green's functions by equations (19) and (20). In this section we develop a simple algorithm for evaluating these integrals using the numerically determined Green's functions. Discretising the problem and using a time step h (in days), to a good approximation the case of a continuous input can be solved by representing the ²²²Rn flux as a series of discrete inputs $I_m = \phi \mathcal{F}_m h$ at the beginning of each time interval $(m-1)h < t < mh$ where F_m is the mean flux during that time interval and ϕ a small correction factor to compensate for any errors in the inventory at time $t = mh$ due to radioactive decay during the time step. From equation (16), the ²²²Rn distribution in the column at time $t = nh$ (the end of the n th time interval) due to input at the beginning of the m th time interval (time $t = (m-1)h$) is then

$$I_m e^{-\lambda_{Rn}(n-m+1)h} \frac{1}{\sqrt{\pi D(n-m+1)h}} e^{-\frac{z^2}{4D(n-m+1)h}} = I_m G_{Rn}(z, (n-m+1)h). \tag{A1}$$

Assuming a constant flux during each time step the correction factor will be

$$\phi = \frac{1}{\lambda_{Rn} h} (e^{-\lambda_{Rn} h} - 1) \approx 1 + \frac{1}{2} \lambda_{Rn} h \text{ for values of } h < 1 \text{ day} \tag{A2}$$

The correction is ~10% if $h = 1$ d and ~1% if $h = 0.1$ d. Summing the contributions from all inputs during time intervals 1 through n the ²²²Rn concentration in the column at time $t = nh$ is

$$C_{Rn}(z, nh) = \sum_{m=1}^n I_m G_{Rn}(z, (n-m+1)h) = I_1 G_{Rn}(z, nh) + I_2 G_{Rn}(z, (n-1)h) + \dots + I_n G_{Rn}(z, h). \tag{A3}$$

In the same way, the ²¹⁰Pb, ²¹⁰Bi and ²¹⁰Po distributions at time $t = nh$ are

$$C_{Pb}(z, nh) = \sum_{m=1}^n I_m G_{Pb}(z, (n-m+1)h) = I_1 G_{Pb}(z, nh) + I_2 G_{Pb}(z, (n-1)h) + \dots + I_n G_{Pb}(z, h), \tag{A4}$$

$$C_{Bi}(z, nh) = \sum_{m=1}^n I_m G_{Bi}(z, (n-m+1)h) = I_1 G_{Bi}(z, nh) + I_2 G_{Bi}(z, (n-1)h) + \dots + I_n G_{Bi}(z, h), \tag{A5}$$

$$C_{Po}(z, nh) = \sum_{m=1}^n I_m G_{Po}(z, (n-m+1)h) = I_1 G_{Po}(z, nh) + I_2 G_{Po}(z, (n-1)h) + \dots + I_n G_{Po}(z, h), \tag{A6}$$

where $G_{Pb}(z,s)$, $G_{Bi}(z,s)$, $G_{Po}(z,s)$ are the (numerically determined) ²¹⁰Pb, ²¹⁰Bi and ²¹⁰Po Green's functions.

Implementation

Calculations were carried using the MATHEMATICA software package. Assuming that the atmosphere has a vertical height of 30 km divided into 1 km steps, the four Green's functions were stored as arrays

$$GRN(31, N), \quad GPB(31, N), \quad GBI(31, N), \quad GPO(31, N),$$

where N is the total number of time steps in the calculation. The values of GRN were calculated exactly using the formula

$$GRN(i, j) = G_{Rn}(i, jh) = e^{-\lambda_{Rn} jh} \frac{1}{\sqrt{\pi D j h}} e^{-\frac{z^2}{4 D j h}}. \tag{A7}$$

The values of GPB, GBI, GPO were evaluated from the numerically determined Green's functions

$$GPB(i, j) = G_{Pb}(i, jh), \quad GBI(i, j) = G_{Bi}(i, jh), \quad GPO(i, j) = G_{Po}(i, jh). \tag{A8}$$

The ²²²Rn exhalation rates were stored as a vector array $F(N)$, where $F(j)$ is the input at the beginning of the j th time step. The concentration profiles were stored in arrays

$$CRN(31, N), \quad CPB(31, N), \quad CBI(31, N), \quad CPO(31, N)$$

where $CRN(i, j)$, $CPB(i, j)$, $CBI(i, j)$, $CPO(i, j)$ are the radionuclide concentrations at altitude $z = i$ at the end of the j th time step. The entries for these arrays were calculated using the formulae

$$\left. \begin{aligned} CRN(i, j) &= \sum_{k=1}^j F(k) GRN(i, j-k+1) \\ CPB(i, j) &= \sum_{k=1}^j F(k) GPB(i, j-k+1) \\ CBI(i, j) &= \sum_{k=1}^j F(k) GBI(i, j-k+1) \\ CPO(i, j) &= \sum_{k=1}^j F(k) GPO(i, j-k+1) \end{aligned} \right\}. \tag{A9}$$

Using these equations, a numerical solution can be constructed for any given distribution of the ²²²Rn exhalation rate $\mathcal{F}(t)$, any given value of the removal rate constant κ , and any desired number of time steps N .

Global equilibrium distributions

The steady state distribution in a column moving from west to east will include steady state contributions from each part of the Earth's surface it passes over. In particular, dividing the global circulation time T into N time steps $h = T/N$, the input during the m th time step can be approximated by a source of strength $I_m = \phi \mathcal{F}_m h$

where \mathcal{F}_m is the value of the exhalation rate at time $s = (m-1)h$, the beginning of the m th time step. Noting that the equilibrium Green's function is periodic of period T the contribution of exhalation from this geographical location to the equilibrium ^{222}Rn distribution in the column at time $t = nh$, the end of the n th time step, can be written

$$I_m G_{Rn}^{equ}(z, t + T - s) = I_m G_{Rn}^{equ}(z, (n + N - m + 1)h)$$

The equilibrium ^{222}Rn distribution at time $t = nh$ due to inputs from all N steps is thus

$$C_{Rn}(z, nh) = \sum_{m=1}^N I_m G_{Rn}^{equ}(z, (n + N - m + 1)h). \quad (A10)$$

The distributions of the daughter radionuclides ^{210}Pb , ^{210}Bi and ^{210}Po can similarly be written

$$\left. \begin{aligned} C_{Pb}(z, nh) &= \sum_{m=1}^N I_m G_{Pb}^{equ}(z, (n + N - m + 1)h) \\ C_{Bi}(z, nh) &= \sum_{m=1}^N I_m G_{Bi}^{equ}(z, (n + N - m + 1)h) \\ C_{Po}(z, nh) &= \sum_{m=1}^N I_m G_{Po}^{equ}(z, (n + N - m + 1)h) \end{aligned} \right\} \quad (A11)$$

Implementation

The four equilibrium Green's functions were stored as arrays over two cycles

$$\text{EGRN}(31, 2N), \quad \text{EGPB}(31, 2N), \quad \text{EGBI}(31, 2N), \quad \text{EGPO}(31, 2N)$$

where N is the number of time steps in each cycle,

$$\text{EGRN}(i, j) = G_{Rn}^{equ}(i, jh),$$

and

$$\begin{aligned} \text{EGPB}(i, j) &= G_{Pb}^{equ}(i, jh), \quad \text{EGBI}(i, j) = G_{Bi}^{equ}(i, jh), \quad \text{EGPO}(i, j) \\ &= G_{Po}^{equ}(i, jh). \end{aligned}$$

The ^{222}Rn exhalation rates were stored as a vector array $F(N)$ where $F(j)$ is the input at the beginning of the j th time interval. The equilibrium concentration profiles were stored in arrays

$$\text{ECRN}(31, N), \quad \text{CPB}(31, N), \quad \text{ECBI}(31, N), \quad \text{ECPO}(31, N)$$

where $\text{ECRN}(i, j)$, $\text{ECPB}(i, j)$, $\text{ECBI}(i, j)$, $\text{ECPO}(i, j)$ are the radionuclide concentrations at altitude $z = i$ at time j , the end of the j th time interval. The entries for these arrays were calculated using the formulae

$$\text{ECRN}(i, j) = \sum_{k=1}^N F(k) \text{EGRN}(i, j + N - k + 1),$$

$$\text{ECPB}(i, j) = \sum_{k=1}^N F(k) \text{EGPB}(i, j + N - k + 1),$$

$$\text{ECBI}(i, j) = \sum_{k=1}^N F(k) \text{EGBI}(i, j + N - k + 1),$$

$$\text{ECPO}(i, j) = \sum_{k=1}^N F(k) \text{EGPO}(i, j + N - k + 1).$$

References

Appleby, P.G., Piliposian, G.T., 2010. The origins of ^{210}Pb in the atmosphere and its deposition on and transport through catchment lake systems. In: Hanrahan, G. (Ed.), *Advanced Topics in Environmental Science Volume II: Modelling of Pollutants in Complex Environmental Systems*. ILM Publications, St Albans, pp. 381–404.

Baskaran, M., 2011. Po-210 and Pb-210 as atmospheric tracers and global atmospheric Pb-210 fallout: a review. *J. Environ. Radioact.* 102, 500–513.

Burton, W.M., Stewart, N.G., 1960. Use of long-lived natural radioactivity as an atmospheric tracer. *Nature* 186, 584–589.

Carvalho, F.P., 1995. Origins and concentrations of ^{222}Rn , ^{210}Pb , ^{210}Bi and ^{210}Po in surface air at Lisbon, Portugal, at the Atlantic edge of the European continental landmass. *Atmos. Environ.* 29, 1809–1819.

Feichter, J., Brost, R.A., Heimann, M., 1991. Three-dimensional modelling of the concentration and deposition of ^{210}Pb aerosols. *J. Geophys. Res.* 96 (D12), 22447–22460.

Gavini, M.B., Beck, J.N., Kuroda, P.K., 1974. Mean residence times of the long-lived radon daughters in the atmosphere. *J. Geophys. Res.* 79, 4447–4452.

Israël, H., 1951. Radioactivity of the atmosphere. In: Malone, T.F. (Ed.), *Compendium of Meteorology*. Amer. Meteor. Soc., Boston, pp. 155–161.

Jacobi, W., André, K., 1963. The vertical distribution of radon 222, radon 220 and their decay products in the atmosphere. *J. Geophys. Res.* 68 (13), 3799–3814.

Junge, C.E., 1962. Note on the exchange rate between the northern and southern atmosphere. *Tellus XIV*, 242–246.

Liu, H., Jacob, D.J., Bey, I., Yantosca, R.M., 2001. Constraints from ^{210}Pb and ^7Be on wet deposition and transport in a global three-dimensional chemical tracer driven model driven by assimilated meteorological fields. *J. Geophys. Res.* 79, 4447–4452.

Monaghan, M.C., 1989. Lead-210 in surface air and soils from California: implications for the behaviour of trace constituents in the planetary boundary layer. *J. Geophys. Res.* 94D, 6449–6456.

Moore, H.E., Poet, S.E., Martell, E.A., 1973. ^{222}Rn , ^{210}Pb , ^{210}Bi and ^{210}Po profiles and aerosol residence times versus altitude. *J. Geophys. Res.* 78, 7065–7075.

Moore, H.E., Poet, S.E., Martell, E.A., Wilkening, M.H., 1974. Origin of ^{222}Rn and its long-lived daughters in air over Hawaii. *J. Geophys. Res.* 79, 5019–5024.

Peirson, D.H., Cambay, R.S., Spicer, G.S., 1966. Lead-210 and polonium-210 in the atmosphere. *Tellus* 18, 427–433.

Piliposian, G.T., Appleby, P.G., 2003. A simple model of the origin and transport of ^{222}Rn and ^{210}Pb in the atmosphere. *Contin. Mech. Thermodyn.* 15, 503–518.

Poet, S.E., Moore, H.E., Martell, E.A., 1972. Lead 210, bismuth 210 and polonium 210 in the atmosphere: accurate ratio measurement and application to aerosol residence time determination. *J. Geophys. Res.* 77, 6515–6527.

Rasch, P.J., Feichter, J., Law, K., et al., 2000. A comparison of scavenging and deposition processes in global models: results from the WCRP Cambridge workshop of 1995. *Tellus* 52B, 1025–1056.

Rehfeld, S., Heiman, M., 1995. Three dimensional atmospheric transport simulation of the radioactive tracers ^{210}Pb , ^7Be , ^{10}Be , and ^{90}Sr . *J. Geophys. Res.* 100, 26141–26161.

Turekian, K.K., Nozaki, Y., Benninger, L.K., 1977. Geochemistry of atmospheric radon and radon products. *Ann. Rev. Earth Planet. Sci.* 5, 227–255.

Warneck, P., 2000. *Chemistry of the Natural Atmosphere*. Academic Press, 927 pages.

Wilkening, M.H., Clements, W.E., 1975. Radon 222 from the ocean surface. *J. Geophys. Res.* 80, 3828–3830.